Published by IOP Publishing for Sissa Medialab

Received: *October 14, 2019*
Accepted: *November 25, 2019*
Published: *January 16, 2020*

21st International Workshop on Radiation Imaging Detectors
7–12 yJuly 2019
Crete, Greece

A UV photodetector based on ordered free standing MWCNT

A. Kyriakis,[a,1] **N. Glezos,**[b] **D. Velessiotis,**[b] **G. Pilatos,**[b] **T. Speliotis**[b] **and A. Stefanou**[c]

[a] *Institute of Nuclear and Particle Physics, NCSR "Demokritos", AgiaParaskevi, Athens 15310, Greece*
[b] *Institute of Nanoscience and Nanotechnology, NCSR "Demokritos", AgiaParaskevi, Athens 15310, Greece*
[c] *National Technical University of Athens, IroonPolytexneiou 9, 157 80 Athens, Greece*

E-mail: kyriakis@inp.demokritos.gr

Abstract: Multiple wall carbon nanotubes (MWCNT) present advantages for optoelectronic applications such as the large effective photo-collector surface as well as the possibility to tune their band gap and absorbance through the growth parameters. The combination of CNTs with conventional semiconductors and metals to form a device presents technological challenges because of the high temperatures required for the production of CNTs and the catalysts used (e.g. Fe). These conditions may result in structural modifications of the substrate specially when the CNT formation temperature approaches the formation temperatures of other layers or even cause metal migration. The use of ordered free-standing MWCNTs for photodevice presents advantages, since they have a tunable absorbance depending on their height while their dense ordering results in a large effective area sensor. Additionally, the bandgap depends on their thickness, thus it is tunable by changing the formation conditions. In this work, we demonstrate a hybrid MWCNT/Si_3N_4/n-Si photodetector based on ordered MWCNTs and evaluate its performance in the UV, visual and near IR spectrum (200–1000 nm). Depending on the application the absorbing nanotube layer can be made thick enough (e.g. several millimeters) to enhance radiation absorption and electron-hole pair generation. The best result obtained so far as a UV detector is a 90% Equivalent Quantum Efficiency @ 275 nm for a 20 μm CNT layer thickness.

Keywords: Photon detectors for UV, visible and IR photons (solid-state); Photon detectors for UV, visible and IR photons (solid-state) (PIN diodes, APDs, Si-PMTs, G-APDs, CCDs, EBCCDs, EMCCDs, CMOS imagers, etc)

[1] Corresponding author.

https://doi.org/10.1088/1748-0221/15/01/C01015

2020 JINST 15 C01015

Contents

2020 JINST 15 C01015

1 Introduction

Carbon nanotubes (CNT) have attracted great interest for applications because of their unique mechanical, electronic and optoelectronic properties. In the latter field, the fabrication of optoelectronic devices on silicon substrates using multiple wall carbon nanotubes (MWCNT) presents high scientific and technological interest. Devices with a MWCNT component [1, 2] or combinations with graphene [3] have already appeared in the literature. Several geometries such as planar metal-semiconductor-metal (MSM) or vertical metal-insulator-semiconductor (MIS) structures have been tested. Due to the size of the MWCNT bandgap, the infrared part of the spectrum has attracted particular attention [2, 4, 5].

There are actually two discrete methods to integrate CNTs in a working device. The most common is to prepare the CNTs separately in solution [6, 7] and then integrating it on the device either by spin coating or by spreading or dipping the substrate in the solution. This approach offers the possibility of miniaturization through the use of conventional nanolithographic techniques and because of its compatibility with the other CMOS processes used during the device fabrication (oxide growth, etching, electrode formation etc.). The drawback of this method is that the resulting devices present low responsivity(R) due to the low density of the sparse CNT film. The second method is to grow an ordered free-standing CNT film directly on the final substrate (semiconductor or glass)through Chemical Vapor Deposition(CVD). In the case of the use of a semiconductor substrate this approach presents significant technological challenges. The growth requires high temperatures (~800°C) and the use of a catalyst (e.g. Fe). However, the use of ordered free-standing MWCNTs for photodevices [8] presents several advantages too: (a) their absorbance can be controlled since it depends upon the film thickness(b) their ordering results in a large effective area sensor and (c) the bandgap is also tunable since it depends upon the formation conditions.

The objective of this work is to realize novel photodetectors based on densely ordered vertical arrays of MWCNTs deposited directly on a Silicon substrate. To this end, it is necessary to match the high temperature (~850°C) CNT formation process with the other processes required for device fabrication. Since a Fe catalyst (Ferrocene) is required during the growth stage, the presence of a diffusion barrier between the MWCNT layer and Si is mandatoryand this is the principal reason for including theSi_3N_4layer. Actually, the nitride layer serves multiple purposes (a) it acts as a diffusion

barrier for the Fe atoms of the catalyst inhibiting them from migrating in the silicon substrate, as already stated, (b) renders the device sensitive in the UV region, because of its large bandgap (5.2 eV) and (c) serves as an anti-reflecting coating as well as a dark current reducer. The MWCNT layer acts as an effective photon absorber and electron-hole generation takes place in the substrate including the silicon nitride layer.

2 Device fabrication

The device cell structure is presented in figure 1. The device cells are fabricated on an n-type (100) Si wafer (450 μm thickness) of $\rho = 10\,\Omega\cdot$ cm. The back plain of the cell is covered with a thin (100 nm) electrode of gold (Au), while a 150 nm Si_3N_4 layer is deposited on the top surface via CVD. This is followed by the growth of the CNT layer in the form of a disk of 6 mm diameter via Catalytic CVD and the thermal evaporation of an aluminum (Al) thin (100 nm) electrode of diameter 2.5 mm through a stencil mask. This device which in sequence will be referred as the "detector" has the series of layers (from bottom to top face) Au/n-Si/Si_3N_4/MWCNT/Al. In all measurements we compare this to a sample not processed for CNT formation ("blank": Au/n-Si/Si_3N_4/Al) and to a sample thermally processed for CNT growth in the presence of the Fe catalyst but with the nanotubes removed ("CNT removed": Au/n-Si/Si_3N_4/thermal process/Al). Thus, it is possible to address the role of the MWCNT layer in the band diagram of the device as well as to investigate the modification of the nitride layer by the Fe catalyst.

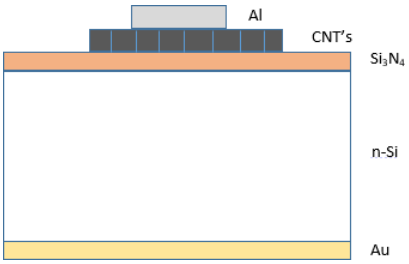

Figure 1. Device cell Structure.

The reactor used for the CNT development is displayed in figure 2. A mixture of 2 g of Camphore with 0.1 g of Ferrocene as a catalyst was injected into the deposition chamber with the use of N_2 gas flow (0.6l/min), after preheating at 200°C. The mixture gas travels through the main high temperature oven, which is kept at $\theta = 850$°C and MWCNTs are formed on the "cold" substrate. The whole process lasts about 40 min and produces well-ordered MWCNTs (figure 3).

3 Results and discussion

The nitride layer plays an important role in this device and this is manifested by electrical and optical measurements. The 'blank' device when voltage biased (top electrode positive) presents low conductance (figure 4, dotted black line) in both directions. A possible transport mechanism is trap assisted tunneling within the nitride layer. This conductance is almost constant in the voltage region (−3 V, 2 V) and increases for more negative values (reverse biasing, top electrode negative). This increase is attributed to the Au/n-Si bottom contact, which is forward biased in this case.

2020 JINST 15 C01015

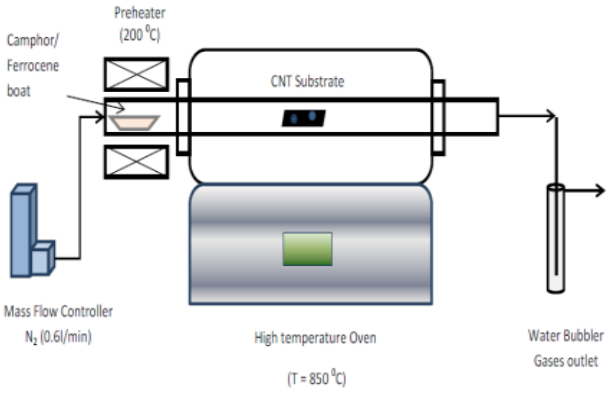

Figure 2. The CNT development facility with the High Temperature Oven.

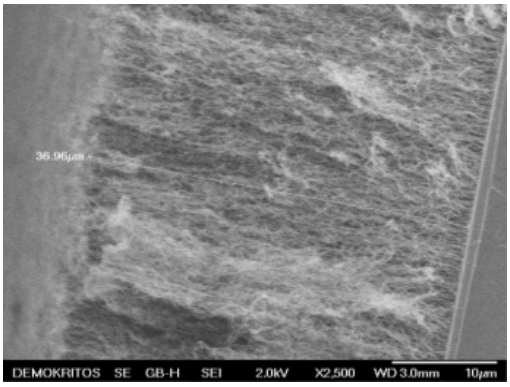

Figure 3. MWCNTs of 20μm in length and 15 nm in diameter.

When the device cells are thermally treated in the stage of CNT deposition the Fe catalyst atoms contaminate the nitride layer and the conductance behavior completely changes. The fabricated detector behaves as a Schottky diode (figure 4, red solid line) that depends upon the MWCNT/n-Si barrier. In this case the nitride layer, due to the addition of the Fe traps, becomes a series resistance manifesting itself as a bending of the forward characteristic (bias >0.5 V). This resistance was measured in the range 10–30kOhm for different lots of devices. The "CNT removed" reference is also a Schottky diode dependent on the Al/n-Si barrier. The barrier height of the detector has been calculated by different methods [9] and its value is 0.54±0.02 eV. The quality factor of the Schottky diode with the series resistance included is of the order of $\eta \sim 1.5$.

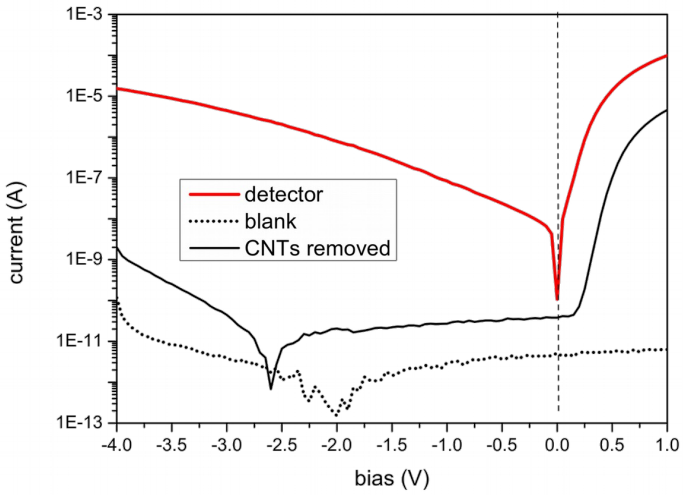

Figure 4. The current /voltage characteristic of the detector compared to reference samples.

The trapping role of the Fe atoms is also demonstrated in capacitance/voltage measurements. In figure 5, the admittance over omega (G/ω) vs frequency (f) is plotted in the case of the "blank" and the "CNT removed" references. The Fe traps contribute by a time constant of 56μsec affecting the performance of the device.

2020 JINST 15 C01015

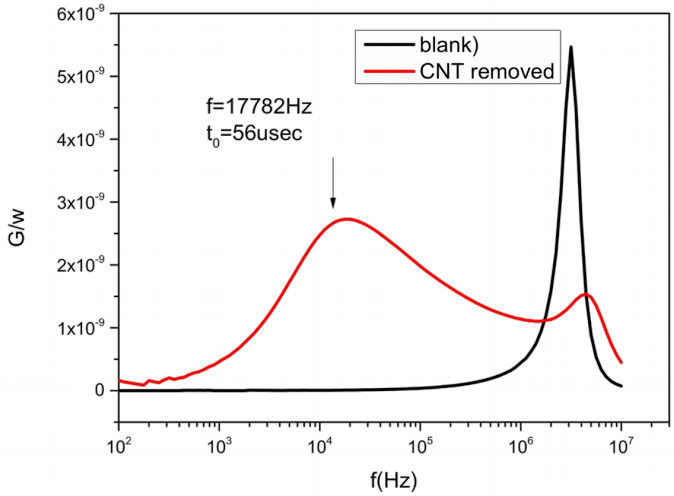

Figure 5. The CNT formation procedure requires the presence of Fe catalyst. This is blocked by the Si_3N_4 layer resulting in donor/acceptor traps with a characteristic time of 56μsec.

The optical response of the device depends both on the MWCNTs as well as on the presence of the nitride layer. The bandgap of MWCNTs is in the IR region and known applications have focused there [10, 11]. However, in our case the nanotubes act as a UV photon absorber. In fact, ordered arrays of MWCNTs absorb equally well in the UV part of the spectrum as in the visible and NIR [12]. Electron-hole generation starts at the interface with the nitride layer. The UV response of the device is attributed to the presence of the nitride layer which has a bandgap of ~5.2 eV (238 nm).

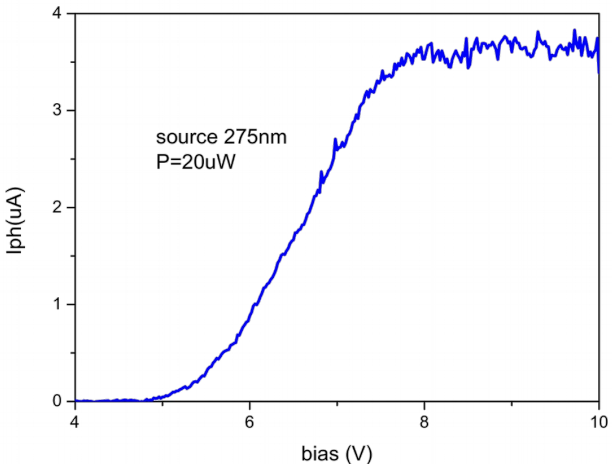

Figure 6. UV response of the device vs bias voltage.

When used as a photodetector, the device is biased in the inverse direction (n-Si substrate positive). The optical features of the detector were tested with a monochromatic source at 275 nm. This value was selected because (a) it is close to the bandgap value of the nitride and (b) the absorbance of the MWCNT layer is high. In the example presented in figure 6 the device has an onset at 5 V bias. The responsivity(R) of this device at 8 V bias and 20 μW source power is

2020 JINST 15 C01015

140 mA/W. Using the same source and several device cells we have covered an optical power range of 0.1 μW – 200 μW. At low source power (0.3 μW) and 7.0 V bias, we found a peak responsivity of 200 mA/W corresponding to 90% equivalent quantum efficiency (EQE). For higher voltage biases the response decreases. This saturation effect is also power dependent. Beyond a specific power value which is bias dependent the photocurrent does not increase further with the increase of the incident power. The responsivity values reported here are at the same level as those of the best performing Schottky or MSM type GaN, UV detectors [13].

Besides the responsivity there are other figures of merit for a photodetector related to time response such as the Noise Equivalent Power (NEP) and the detectivity(D^*) [14]. As an example, a disordered MWCNT layer combined with graphene has demonstrated a high detectivity of $1.5 \cdot 10^7$ cm $Hz^{1/2}$/W in IR [15] still lower than III-V devices. A rough estimation of the expected detectivity can be made using the data presented in this work. Assuming that the presence of the Fe traps is the most important limiting factor on the sampling bandwidth Δf, we select $\Delta f = 17.8$ kHz (figure 5). The noise level at 8 V (figure 6) is $I_n = 0.08$ μA, the device area is 0.25 cm^2. Plugging the aforementioned values to the detectivity equation $D^* = \sqrt{A \cdot \Delta f} \cdot R/I_n$, we obtain a value of $11.7 \cdot 10^7$ cm $Hz^{1/2}$/W, where for responsivity $R = 140$ mA/W. A more accurate evaluation under various operating conditions is the objective of future work.

4 Conclusions

We fabricated metal-semiconductor photodetectors based on standing carbon nanotubes developed by Catalyst CVD. A low conductance silicon nitride layer containing Au and Fe traps deposited during the process was used to reduce the inverse bias dark current and act as a diffusion barrier to protect the Si substrate. The optical responsivity values obtained at the UV part of the spectrum as well as the estimation of the detectivity of the examined devices indicate that hybrid MWCNT/Si_3N_4/n-Si systems have a potential for UV photodetector applications.

Acknowledgments

This project has received funding from the Hellenic Foundation for Research and Innovation (HFRI) and the General Secretariat for Research and Technology (GSRT), under grant agreement No 157446/I2/21-9-2018.

References

[1] P. Ong, W.B. Euler and I.A. Levitsky, *Carbon nanotube-Si diode as a detector of mid-infrared illumination*, *Appl. Phys. Lett.* **96** (2010) 033106.

[2] L. Xiao et al., *A polarized infrared thermal detector made from super-aligned multiwalled carbon nanotube films*, *Nanotechnology* **22** (2010) 025502.

[3] R. Lu, C. Christianson, B. Weintrub and J.Z. Wu, *High photoresponse in hybrid graphene-carbon nanotube infrared detectors*, *ACS Appl. Mater. Interfaces* **5** (2013) 11703.

[4] Y. An, H. Rao, G. Bosman and A. Ural, *Characterization of carbon nanotube film-silicon Schottky barrier photodetectors*, *J. Vac. Sci. Tech.* **B 30** (2012) 21805.

[5] F. Rao, X. Liu, T. Li, Y. Zhou and Y. Wang, *The synthesis and fabrication of horizontally aligned single-walled carbon nanotubes suspended across wide trenches for infrared detecting application*, *Nanotechnology* **20** (2009) 055501.

[6] D. Melisi et al., *Radiation detectors based on Multiwall Carbon Nanotubes deposited by a spray technique*, *Thin Solid Films* **543** (2013) 19.

[7] D. Melisi et al., *Photodetectors based on carbon nanotubes deposited by using a spray technique on semi-insulating gallium arsenide*, *Beilstein J. Nanotechnol.* **A 5** (2014) 1999.

[8] C. Aramo et al., *Progress in the realization of a silicon-CNT photodetector*, *Nucl. Instrum. Meth.* **A 695** (2012) 150.

[9] A. Filatzikioti et al., *Carbon nanotube Schottky type photodetectors for UV applications*, *Solid State Electron.* **151** (2019) 27.

[10] M. Richter, T. Heumuller, G.J. Matt, W. Heiss and C.J. Brabec, *Carbon Photodetectors: The Versatility of Carbon Allotropes*, *Adv. Energy Mater.* **7** (2016) 1601574.

[11] X. He, F. Leonard and J. Kono, *Uncooled Carbon Nanotube Photodetectors*, *Adv. Opt. Mater.* **3** (2015) 989.

[12] T. Zhang, Z. Chen and B. Tang, *Nonlinear Optical Property of Aligned Multi-Walled Carbon Nanotube Film*, in proceedings of the *2009 Symposium on Photonics and Optoelectronics*, Wuhan, China, 14–16 August 2009, [DOI].

[13] Z. Alaie, S.M. Nejad and M.H. Yousefi, *Recent advances in ultraviolet photodetectors*, *Mater. Sci. Semicond. Process.* **29** (2015) 16.

[14] C.-H. Lin and C.W. Liu, *Metal-Insulator-Semiconductor Photodetectors*, *Sensors* **10** (2010) 8797.

[15] A. Rogalski, *Infrared detectors: status and trends*, *Prog. Quantum Electron.* **27** (2003) 59.

2020 JINST 15 C01015